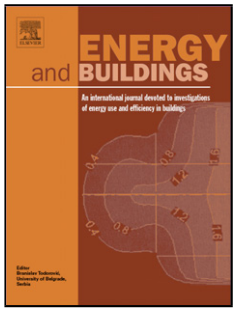

Title: Thermal delay provided by floors containing layers that incorporate expanded cork granule waste

Author: A. Tadeu A. Moreira J. António N. Simõ es I. Simõ es

PII: S0378-7788(13)00653-1
DOI: http://dx.doi.org/doi:10.1016/j.enbuild.2013.10.007
Reference: ENB 4572

To appear in: *ENB*

Received date: 24-6-2013
Revised date: 3-9-2013
Accepted date: 6-10-2013

Please cite this article as: A. Tadeu, A. Moreira, J. António, N. Simõ es, I. Simõ es, Thermal delay provided by floors containing layers that incorporate expanded cork granule waste, *Energy and Buildings* (2013), http://dx.doi.org/10.1016/j.enbuild.2013.10.007

Thermal delay provided by floors containing layers that incorporate expanded cork granule waste

A. Tadeu[a,*], A. Moreira[b], J. António[a], N. Simões[a], I. Simões[c]

[a] Department of Civil Engineering, Faculty of Sciences and Technology, University of Coimbra, Pólo II, Rua Luís Reis Santos, 3030-788 Coimbra, Portugal
* Corresponding author: e-mail addresses: tadeu@dec.uc.pt; phone: 00351239798949

[b] Polytechnic Institute of Tomar, Campus Tomar, Quinta do Contador, 2300-313 Tomar, Portugal

[c] ITeCons Rua Pedro Hispano, 3030-289 Coimbra, Portugal

Abstract

This paper reports the computation of the thermal delay provided by concrete floors built with layers of cork and lightweight screed that incorporate expanded cork granule waste. The heat transfer by conduction across these multilayer systems is simulated analytically under unsteady boundary conditions.

The thermal delay is computed for multilayer concrete floors with varying numbers of layers and layer thicknesses. The mass density and thermal conductivity of the various materials were determined experimentally. Given its heterogeneity, the specific heat of the lightweight screed was obtained indirectly using both the experimental results and the analytical model.

The results obtained show the potential of these composites in applications for increasing the thermal performance of concrete floors, in particular the thermal delay and thermal resistance. The results show that the contribution of the insulating lightweight screed material's properties to thermal delay is more relevant in systems composed of few layers. The constructive solutions composed of a greater number of layers present higher thermal delay value.

Key words: *Transient heat conduction; thermal delay, analytical solutions, frequency domain, building multilayer floors; expanded cork*

1. Introduction

Heating and cooling energy requirements have become more important in recent decades, as borne out by the policies that are being implemented (e.g. Directive 2010/31/EU of the European parliament on the energy performance of buildings [1]). The energy performance of a building is influenced by several factors, such as indoor and outdoor climate conditions, design, thermal characteristics of the building envelope, internal loads (solar and internal heat gains) and HVAC (heating ventilation and air-conditioning) systems. The design of a passive building

must consider certain parameters in order to provide good thermal comfort conditions for users for the lowest heating energy cost [2]. The building envelope is one of these parameters since it significantly affects the indoor conditions [2]. Researchers have therefore been studying the thermal properties of building elements in order to understand how they contribute to interior comfort for the lowest life cycle cost [2] and to define the thermal performance of occupied and naturally ventilated houses [3]. Pereira et al. [3] investigated the correlations between the percentage of discomfort hours and the equivalent thermal transmittance, thermal capacity and thermal delay values of the envelope's components. They concluded that the number of discomfort hours is lower in buildings with a higher thermal capacity and thermal delay envelope values, and that the thermal property with the best correlation to discomfort hours is thermal capacity. The transmission rate of heat transfer through the envelope elements that separate the air-conditioned space and the outside air depends on how the thermal bridges are dealt with [4] and on the insulation level of the flat envelope. Under steady state conditions the building envelope should provide high thermal resistance. However, as real conditions are mostly unsteady, in addition to providing good thermal resistance building elements should have the thermal capacity to attenuate and delay external temperature fluctuations. Simões et al. [5] used an analytical model, validated with experimental results, to show the importance of cork layers in the thermal delay conferred by multilayer wall systems. Mathieu-Potvin and Gosselin [6] computed numerically the thermal shielding exhibited by an exterior wall containing layers of PCMs. Yilmaz [7] evaluated the thermal performance of two buildings, in order to show the importance of thermal mass in hot dry climates.

The flat opaque elements are characterized taking into consideration both the thermal transmittance (U-value) and their thermal capacity ([8], [9]). In fact, over the last few years thermal capacity is increasingly cited as an important saving energy aspect that also improves a building's comfort levels ([8]-[12]). Greater thermal capacity enables indoor thermal comfort to be achieved using less energy for climate control.

Thermal delay is one of the parameters that may be used to predict the dynamic thermal behaviour of building elements [8]. Antonopoulos and Tzivanidis [13] defined thermal delay as the time needed for the mean indoor air temperature to rise above the mean value of the outdoor temperature oscillations by a specified amount under specified building heating. Their paper proposes a finite-difference solution of a system of coupled differential equations describing the transient heat transfer and energy balance in buildings; this is used to calculate the time delay for a wide range of climate conditions and a variety of fully-insulated and non-insulated buildings. Few years later, Antonopoulos and Koronaki [12] presented a procedure for estimating the thermal delay of typical buildings in which the effect of the indoor mass provided by partitions and furnishings was examined. They demonstrated that the indoor mass promotes an increase of up to 40 percent in thermal delay. In another work, [8], the same authors correlated the dynamic parameters, i.e. the effective thermal capacitance, the time constant and the thermal delay, in terms of the thickness of exterior wall layers and the percentage of every envelope element. They concluded that knowing the thermal contribution of each part of the

envelope is important to improve the prediction of the dynamic thermal behaviour of buildings in the design phase. Kravvaritis *et al*. [15] developed a 'thermal delay method' based on the 'T-history' method used to measure the thermal properties of phase change materials (PCMs). The proposed method was used to measure PCMs' thermophysical properties, i.e. phase change heat, temperature and the corresponding heat capacities. Simões *et al.* [5] presented an analytical formulation to compute thermal delay in multilayer systems with insulating materials, such as cork, mineral wool and expanded polystyrene. The results prove that the contribution of the insulating material's properties to thermal delay is more relevant in systems composed of few layers. The same study shows that a longer thermal delay occurs for construction solutions composed of layers with low overall thermal diffusivity and larger insulation thickness.

Multilayer systems composed of different materials seem to be a rational choice for use in the building envelope, particularly when thermally and acoustically optimized solutions are required ([12], [16]-[17]). Additionally, the current environmental context demands energy conservation along with the use of low impact materials with high technical performance [19]. Cork, as a natural resource that is renewable and recyclable, fulfils these requirements [20]. Cork is obtained from the bark of the cork oak, Quercus Suber L., and is a low density material with excellent thermal and acoustic properties. It can be used in cork-gypsum composite in partitions [21], for stoppers and insulation corkboards [22, 24], in a cement paste [23], cork agglomerates [25, 27], cork-gypsum decorative materials [26] and sandwich panels[28].

Furthermore, in granular form cork waste can also be used as aggregate in lightweight concrete mixtures ([29]-[30]), offering solutions with improved thermal and acoustics properties.

The work described here computes the thermal delay provided by floors containing cork and lightweight screeds incorporating expanded cork granule waste. It uses one-dimensional analytical solutions where the time variable is catered for by using a frequency domain approach. These solutions have been previously proposed and validated against experimental results by the authors ([5], [31]).The technique uses the Green's functions for harmonic heat plane sources. The solutions are formulated as the combination of surface terms that arise within each layer and at each interface so as to satisfy temperature continuity and normal fluxes between layers.

These transient thermal simulations are applied in various multilayer systems, built up by superimposing layers of concrete, lightweight screed layers incorporating expanded cork granule waste, and layers of expanded cork agglomerate. These multilayer systems are assumed to be subjected to sinusoidal temperature variations at one of the external surfaces.

This paper first briefly describes the analytical model used to simulate the transient heat conduction. Then, the concrete mixtures used are listed and the experimental evaluation of the physical and thermal properties of the materials is presented. The specific heat of the lightweight screed is obtained indirectly by using both the experimental results and the analytical model. Laboratory tests were performed to validate the analytical results. Finally, the

thermal delay is computed for different multilayer systems. The variables studied were the number and type of layers, and the thickness and positioning of the lightweight screed.

2. Analytical solutions

The analytical solutions are briefly explained. A full description of these equations can be found in one of our previous papers [5], where the 3D and the 2.5D solution for multi-layered systems has been proposed and validated against experimental results.

Thus, consider a multilayered system built from a set of m plane layers of infinite extent, as shown in Figure 1. This system is subjected to temperatures t_{0t} and t_{0b} at the top and bottom external surfaces. The layers are assumed to be infinite in the x and z directions. The thermal material properties and thickness of the various layers may differ.

The transient heat transfer by conduction in each layer is expressed by the equation

$$\lambda_j \left(\frac{\partial^2}{\partial y^2} \right) T(t,y) = \rho_j \, c_j \, \frac{\partial T(t,y)}{\partial t}, \tag{1}$$

in which t is time, $T(t, y)$ is temperature, the subscript j identifies the layer, λ_j is the thermal conductivity, ρ_j is the density and c_j is the specific heat. These thermal properties are constant in each layer and do not change from point to point.

The solution is defined in the frequency domain after the application of a Fourier transformation to eqn (1)

$$\left(\frac{\partial^2}{\partial y^2} + \left(\sqrt{\frac{-\mathrm{i}\omega}{\alpha_j}} \right)^2 \right) \hat{T}(\omega, y) = 0, \tag{2}$$

where $\mathrm{i} = \sqrt{-1}$, $\alpha_j = \lambda_j \big/ \left(\rho_j \, c_j \right)$ is the thermal diffusivity of the layer j, and ω is the frequency.

The total heat field is found by adding the surface terms arising within each layer and at each interface, as required to satisfy the boundary conditions at the interfaces, i.e. continuity of temperatures and normal flows between layers.

For the layer j, the heat surface terms on the upper and lower interfaces can be expressed as

$$\tilde{T}_{j1}(\omega, y) = E_{0j} \frac{E_{j1}}{\nu_{0j}} A_{0j}^{t}, \tag{3}$$

$$\tilde{T}_{j2}(\omega, y) = E_{0j} \frac{E_{j2}}{\nu_{0j}} A_{0j}^{b}, \tag{4}$$

where $E_{0j} = \dfrac{1}{\lambda_j}$, $E_{j1} = \mathrm{e}^{-\mathrm{i}\nu_{0j}\left| y - \sum_{l=1}^{l-1} h_l \right|}$, $E_{j2} = \mathrm{e}^{-\mathrm{i}\nu_{0j}\left| y - \sum_{l=1}^{j} h_l \right|}$, $\nu_{0j} = \sqrt{\dfrac{-\mathrm{i}\omega}{\alpha_j}}$ and h_l is the thickness of the layer l. A_{0j}^{t} and A_{0j}^{b} are *a priori* unknown potential amplitudes. A system of $2m$ equations

is derived, by ensuring the continuity of temperatures and heat flows along the $m-1$ interfaces between layers, and by imposing the temperatures $\hat{t}_{0t}$ and $\hat{t}_{0b}$ at the top and bottom external surfaces. $\hat{t}_{0t}$ and $\hat{t}_{0b}$ are obtained by Fourier transformation of t_{0t} and t_{0b} in the time domain. All the terms are organized according to the form

$$\begin{bmatrix} \frac{1}{\lambda_1 \nu_{01}} & \frac{e^{-i\nu_{01}h_1}}{\lambda_1 \nu_{01}} & \dots & 0 & 0 \\ e^{-i\nu_{01}h_1} & -1 & \dots & 0 & 0 \\ \frac{e^{-i\nu_{01}h_1}}{\lambda_1 \nu_{01}} & \frac{1}{\lambda_1 \nu_{01}} & \dots & 0 & 0 \\ \dots & \dots & \dots & \dots & \dots \\ 0 & 0 & \dots & -1 & e^{-i\nu_{0m}h_m} \\ 0 & 0 & \dots & -\frac{1}{\lambda_1 \nu_{0m}} & -\frac{e^{-i\nu_{0m}h_m}}{\lambda_m \nu_{0m}} \\ 0 & 0 & \dots & \frac{e^{-i\nu_{nm}h_m}}{\lambda_m \nu_{0m}} & \frac{1}{\lambda_m \nu_{0m}} \end{bmatrix} \begin{bmatrix} A_{01}^t \\ A_{01}^b \\ \dots \\ A_{0m}^t \\ A_{0m}^b \end{bmatrix} = \begin{bmatrix} \hat{t}_{0t} \\ 0 \\ 0 \\ \dots \\ 0 \\ 0 \\ \hat{t}_{0b} \end{bmatrix} \quad (5)$$

Solving this system gives the amplitude of the surface terms at each interface, leading to the following temperature and heat flux fields at layer j,

$$\tilde{T}(\omega, y) = E_{0j}\left(\frac{E_{j1}}{\nu_{0j}} A_{0j}^t + \frac{E_{j2}}{\nu_{0j}} A_{0j}^b\right) \text{ if } \sum_{l=1}^{j-1} h_l < y < \sum_{l=1}^{j} h_l \,, \quad (6)$$

The problem is recast in the time domain by means of inverse Fourier transforms, using complex frequencies to avoid aliasing. These solutions do not require any type of discretization of the space domain. No restriction is placed on the source time dependence since the static response is obtained by limiting the frequency to zero and ensuring that the high frequency contribution to the response is small. This overcomes some of the limitations posed by other methods that require the use of simplifications such as the discretization of the layer into a large number of identical thin layers ([32], [33])

3. Experimental tests

This section reports the use of an experimental procedure for determining the specific heat of lightweight screed specimens incorporating cork. Given its heterogeneity its specific heat is evaluated indirectly. This is accomplished by recording the temperature variation across multilayer test specimens, built by laying a lightweight screed layer between two moulded expanded polystyrene (EPS) layers and subjecting them to 1D heat conduction. The equipment consisted of a guarded hot plate and a set of thermocouple sensors connected to a data logger system. The systems were subjected to an unsteady heat flow rate. The temperature variation at each interface layer was measured by two thermocouples placed at each system interface, including the top and bottom surfaces, respectively in contact with the heating and cooling plates. The temperature change in the top and bottom surfaces of the multilayer system was used as an input for the semi-analytical model assembled using the thermal properties obtained

experimentally. The measurements were later compared with the analytical solutions using as data the surface temperatures of each multilayer system, the density and thermal conductivity of each material, obtained experimentally. The specific heat value that best fits the experimental results is then selected. This is repeated for lightweight screeds with different cement dosages, with and without expanded cork granules. These tests were carried out at ITeCons - Institute for Research and Technological Development in Construction Sciences, a laboratory that can perform a large number of experimental tests accredited by IPAC - Instituto Português de Acreditação (member of EA: European cooperation for Accreditation; and ILAC: International Laboratory Accreditation Cooperation).

3.1. **Lightweight screed mixtures**

The lightweight screeds (LWSs) were made with Portland cement (CEM II/B-L 32.5 N), natural river sand, expanded cork granules (ECG) and water. The diameters of the cork particles were $3-5\,\mathrm{mm}$ (ECG 3/5) and $5-10\,\mathrm{mm}$ (ECG 5/10), in equal volume proportion. In the LWSs, $80\,\%$ of the natural river sand was replaced by ECG 3/5 and ECG 5/10, in volume. The experiments were carried out using mixes with 3 different cement dosages: $150\,\mathrm{kg.m^{-3}}$ (M150), $250\,\mathrm{kg.m^{-3}}$ (M250) and $400\,\mathrm{kg.m^{-3}}$ (M400). Screed mixtures without any cork content were prepared using the same cement dosage, which were labelled R150, R250 and R400 and used as reference. The specimens were cured in a controlled environment with a set-point temperature of $(23\pm2)\,^{\circ}\mathrm{C}$ and $100\,\%$ relative humidity for 28 days. Table 1 lists the concrete mixtures used.

3.2. Thermal and physical properties

This section describes how the thermal and physical properties of the lightweight screeds, the moulded expanded polystyrene (EPS) and the expanded cork agglomerate (ICB) were evaluated. It first presents the determination of the mass density and thermal conductivity and goes on to describe the procedure used to evaluate the specific heat.

3.2.1. Mass density and thermal conductivity

The EPS and ICB were first characterized to find their thermal conductivity and mass density. The thermal conductivity was found by the guarded hot-plate method (ISO 8302:1991 [34]) using a Lambda-Mebtechnik GmbH Dresden apparatus, single-specimen Lambda-meter EP-500 model, following the test procedure defined in EN 12667:2001 [35]. This equipment was verified for the mean temperatures of 10ºC, 25ºC and 40ºC, using three reference materials, the 'Etalon für Einplattenapparatur EP-500 Mebprotocoll - Nr. Etal8501', 'Institute Reference Materials Measurements - 440 (S64)' and 'National Physical Laboratory - LA472'. The mass density of EPS and ICB was determined using the procedure described in EN 1602:1996 [36].

The density of the LWSs and reference screed specimens was calculated for cubic specimens $(150\times150\times150)\,\mathrm{mm}^3$, in compliance with NP EN 12390-7:2009 [37], at 28 days. Their thermal conductivity was evaluated as defined for the EPS and the ICB.

Table 2 gives the averages of those properties for the different materials used in the experiments and the associated measurement uncertainties.

3.2.2. Specific heat

The specific heat of the ICB and the EPS were obtained with a Netzsch apparatus, model DSC200F3, using the ratio method. A value of $1560.0\pm95.0\,\mathrm{J.kg^{-1}.^oC}$ was found for the ICB and of $1430.0\pm99.0\,\mathrm{J.kg^{-1}.^oC}$ for the EPS.

As mentioned above the specific heat of the lightweight screed and reference screeds was evaluated indirectly. Multilayer systems were built by sandwiching lightweight screed measuring $150\times150\,\mathrm{mm}^2$ between two EPS layers to accommodate any surface irregularity. Each multilayer system thus had 3 layers. Table 3 lists the systems, giving the thickness of each layer and their sequence.

The experiment is based on the application of an unsteady heat flow rate on each multilayer system using the single-specimen Lambda-meter EP-500 apparatus. To mitigate the interface resistance within the test specimen the tests were performed under a constant pressure of $2500\,\mathrm{Pa}$, applied via the equipment plates.

Before running any test the specimens were conditioned in a climatic chamber, Fotoclima 300EC10 from Aralab, with a controlled environment with a set-point temperature of $(23\pm2)\,^o\mathrm{C}$ and $(50\pm5)\,\%$ relative humidity, until constant mass was reached.

The tests were carried out in a controlled laboratory environment where the initial test conditions were a temperature of $(23\pm2)\,^o\mathrm{C}$ and relative of humidity of $(50\pm5)\,\%$. The single-specimen Lambda-meter EP-500 was first programmed to reach a mean temperature of $23\,^o\mathrm{C}$ in the test specimen, establishing a $15\,^o\mathrm{C}$ temperature difference between the heating and the cooling units.

During the heat conduction test, the temperature of the top multilayer surface (in contact with the heating plate unit) rose, while the temperature of the bottom multilayer surface (in contact with the lower plate) fell. In this apparatus, the 1D transfer is guaranteed in a metering area of $150\times150\,\mathrm{mm}^2$ at the centre by using a 'hot ring'. The equipment ensured null heat flows across the lateral faces. The energy input was maintained until a permanent heat flow rate was reached, that is, when there were no temperature variations at the multilayer interfaces. The system then stopped heating and cooling until the initial temperatures were reached again.

The temperature variation at each interface layer and within the test specimen was measured by type T (copper) thermocouples $0.2\,\mathrm{mm}$ thick. Thermocouples were calibrated beforehand by an accredited laboratory. Two thermocouples were placed at each system interface and

within the test specimen, including the top and bottom surfaces, respectively in contact with the heating and cooling plates. The data were recorded using a Yokogawa MW 100 data logger, with a time interval of 10 seconds.

These experimental measurements are then compared with analytical results obtained as described in section 2. The materials' thermal properties, already obtained experimentally (see Table 1), were used in these simulations. The specific heat of the lightweight screed and reference screeds was found by verifying the estimate that leads to the best fit with the experimental temperature measurements.

First, the temperatures $\hat{t}_{0t}$ and $\hat{t}_{0b}$ used in the analytical formulation were defined by applying a direct discrete fast Fourier transform in the time domain to the temperatures recorded by the thermocouples on the external multilayer system, subtracting the initial temperature (T_{initial}). Based on the experimental responses, an analysis period of $40\,\text{h}$ was established, which was enough to find the energy equilibrium of the multilayer system with the environment (temperatures at the different interfaces were again restored almost to the initial test temperatures), for the 1D heat conduction. The upper frequency of the analysis was fixed so that its contribution to the global response was negligible.

The analytical computations were performed in the frequency domain for frequencies ranging from $0.0\,\text{Hz}$ to $\frac{4095}{48\times3600}\,\text{Hz}$, with a frequency increment of $\frac{1.0}{48\times3600}\,\text{Hz}$, which determined a full time analysis window of $48\,\text{h}$.

The temperature variation imposed on the top and bottom multilayer surfaces can be of any type since the static response, corresponding to the frequency $0.0\,\text{Hz}$, can be calculated, given that the use of complex frequencies allows this response to be computed, and the high frequency responses are negligible.

The temperature in the time domain was found by applying a discrete inverse fast Fourier transform in the frequency domain. Aliasing was dealt with by introducing complex frequencies with a small imaginary part, taking the form $\omega_c = \omega - \text{i}\eta$ (where $\omega = 0.7\Delta\omega$, and $\Delta\omega$ is the frequency increment). This shift was subsequently taken into account in the time domain by means of an exponential window, $\text{e}^{\eta t}$, applied to the response. The final temperatures were obtained by adding the initial test temperatures to these responses (T_{initial}).

To illustrate the procedure, the results of the experimental 1D measurements recorded for System 1, test specimen M150, are now presented and compared with those computed analytically. In Figure 2 the black solid lines represent the analytical responses while the experimental measurements are indicated by the lines with marked points (and labelled with the thermocouple number). The experimental results plotted at each interface correspond to the arithmetic mean of the readings from the two thermocouples placed along the x direction, since the heat diffusion is 1D and thus the temperatures recorded at receivers placed at the same position y are similar. This Figure includes only the analytical solution that best fits the

experimental response $\left(c = 950.0\ \mathrm{J.kg^{-1}.^{o}C^{-1}}\right)$. These responses show a good agreement between the semi-analytical responses and the experimental results. The results are similar over the full time window, i.e. when the heating and cooling units are receiving energy, when there is a constant heat flow rate, and when there is no power input. Note that at the beginning of the process all the thermocouples show a temperature similar to the ambient temperature, which satisfies the initial conditions defined for the analytical simulation.

The same procedure was applied to the other systems. Table 4 lists the specific heat values, including the resulting thermal diffusivity. Analysis of these results shows that the specific heat of the screed incorporating cork is higher than those without cork granules. It can further be concluded that the specific heat decreases when the cement content of the mixture is higher.

4. Thermal delay and thermal transmittance coefficient of the floor system

The thermal delay for construction floors made of concrete, expanded cork agglomerate and lightweight screed, incorporating cork was computed as follows. The thermal delay is taken to be the time difference between the instant with the thermal variation at one of the multilayer system's surfaces and the instant it appears at the opposite surface. The temperatures obtained at the receiving surface are computed using the analytical model described above, but previously manipulated so as to include an unbounded medium above.

Four construction system floors were studied, as shown in Figure 3. These systems are composed of a concrete slab $\left(\lambda = 1400.0\ \mathrm{W.m^{-1}.^{o}C^{-1}},\ \rho = 2300.0\ \mathrm{Wkg.m^{-3}},\ c = 880.0\ \mathrm{J.kg^{-1}.^{o}C^{-1}},\ \alpha = 6.92\times10^{-07}\ \mathrm{m^{2}.s^{-1}}\right)$, screed and ICB layers. The thermal insulation is provided by the cork incorporated in the screeds and ICB. Case a (Figure 3a)) is a concrete slab covered with a screed or ICB layer. Case b (Figure 3b)) has an additional floating layer, 30 mm thick, placed over the solution labelled as Case a, and a hard finishing cover is required for it. Case c (Figure 3c)) is composed of a concrete slab covered with a 30 mm thick of screed and an ICB layer. Case d (Figure 3d)), placed over the Case c solution, has an additional floating layer, 30 mm thick. All the systems are subjected to heat diffusion along their normal direction (vertical). So, null heat fluxes are assumed along the horizontal direction. It is assumed that there is no thermal resistance at the layer interfaces, i.e. a continuity of temperatures and heat fluxes is prescribed at those interfaces.

The thermal delay calculations were performed on various thicknesses (e) of the insulation materials, from $15\ \mathrm{mm}$ to $150\ \mathrm{mm}$ (Cases a and b) and from $15\ \mathrm{mm}$ to $120\ \mathrm{mm}$ (Cases c and d), using the thermal and physical properties given above (Tables 1 and 2).

All simulations impose a sinusoidal temperature variation at the bottom surface, simulating the temperature change for a 2-day period, as indicated in Figure 4. The initial temperature in all systems is assumed to be $20\ ^{o}\mathrm{C}$ and to fluctuate by $10\ ^{o}\mathrm{C}$ in each 24-hour period. The medium in contact with the upper receiving surface is assumed to be air $\left(\lambda = 0.026\ \mathrm{W.m^{-1}.^{o}C^{-1}},\right.$

ρ=1.2928 kg.m^{-3}, c=1000.0 J.kg^{-1}.ºC^{-1}). No other thermal resistance at this surface has been included in the model.

The analytical computations were performed in the frequency domain for the frequency range and frequency increment as described above. Figure 5 shows the temperature evolution in the lower exposed surface and the upper receiving surface for Case 1 when the lightweight screed (M150) is 60 mm thick. The solid blue lines correspond to the incident temperature variation and the lines with marked points represent the temperature evolution at the receiving surface (upper surface). The thermal delay is given by the difference between times T2 and T1.

Figure 6 presents the thermal delay (solid lines) and the thermal transmittance coefficient, U (dashed lines), of all the multilayer systems analysed. The left column plots the results obtained when layers of LWS are incorporated in the system or when ICB is used (Figures 6a)-6d)), while the right column relates to systems built with reference screeds (Figures 6e)-6h)).

As expected, these figures show that for all multilayer systems the thermal delay increases and the thermal transmittance decays the thicker the insulation thickness.

Analysis of Figures 6a) and b) indicates that when an ICB layer is used instead of a screed layer or an LWS layer it leads to a longer thermal delay. A maximum difference of about 2 hours is found. The use of LWS layers with lower cement content (i.e. M150 and M250) allows the system to perform better. This is particularly evident in Cases 1 and 2, for a thicker insulation layer and with LWS M150.

Focusing on Case 1 (Figures 6a) and 6e)) and Case 2 (Figures 6b) and 6f)) results, we find that the systems with LWS layers exhibit lower thermal transmittance coefficients than those with the reference screed layers. However, this does not mean a longer thermal delay (e.g. in Case 1 the thermal delay of the system incorporating a layer of M400 is lower than that of R400). Comparing the thermal delay results of Cases 1 and 2, it is evident that the highest values are reached when the screeds are laid under the 30 mm floating concrete slab (Case 2).

Cases 3 (Figures 6c) and 6g)) and 4 (Figures 6d) and 6h)) show that the systems that incorporate the reference screeds exhibit a slightly longer thermal delay than those containing LWS layers. However, it should be noted that the systems with LWSs have lower thermal transmittance coefficients, which confirms that this property is not necessarily a sign of greater thermal delay.

It should be noted that the highest thermal delay values are reached when the screeds (or the ICB) are laid under the 30 mm thick concrete slab: Cases 2 and 4 exhibit greater thermal delays than 1 and 3, respectively, which means that the thermal delay increases with the number of layers, as also reported by Simões *et al*. [5], particularly if those layers differ in terms of their thermal properties. The thermal delay is larger than 3 hours if there is a floating concrete slab.

The presence of the screeds below an ICB layer only represents a slightly higher thermal delay with lower thickness of the ICB layer. This is observed when Case 1 (with ICB) and Case 3 are compared, and when Case 2 (with ICB) and Case 4 are compared. We may conclude that when this type of insulating material is used there is no advantage in using a screed below it.

However, in the absence of the insulating layer, the use of LWSs instead of conventional screeds improves the thermal behaviour of the solution.

It is important to note that the behaviour described above would be similar for different temperature oscillations in terms of thermal delay and thermal transmittance coefficient. The effect of smaller temperature variation amplitudes on the final results is only relevant in terms of the definition of the temperature amplitude variations across the floor systems over time.

5. Conclusions

In this paper we have computed the thermal delay and thermal transmittance coefficient provided by concrete floors built with layers of expanded cork agglomerate and lightweight screeds that incorporate expanded cork granule waste. The lightweight screeds were made with Portland cement in different dosages, sand, expanded cork granules and water. The physical and thermal properties of the lightweight screeds were found experimentally. The specific heat of the lightweight screed has been evaluated indirectly, given its heterogeneity, using both the experimental and analytical simulation results.

The thermal delay was then computed for different multilayer concrete floor systems which contained layers of expanded cork agglomerate and lightweight screed with expanded cork granule waste. The layers' thickness, their number and their position within the system were the variables studied. The results showed that the contribution of the insulating lightweight screed material's properties to thermal delay is more relevant in systems composed of few layers. Longer thermal delays were found in the solution built with a greater number of layers.

The results obtained show the potential for using these layers in floor systems. It has been concluded that their incorporation will lead to a better thermal performance of concrete floors, particularly in terms of thermal delay and thermal resistance. These results for these solutions are even more relevant when compared with other commercial solutions because of their inherent sustainability. Given the low mass density of the proposed solutions it is anticipated that they can be used in retrofit interventions.

6. Acknowledgments

The research work presented herein was supported by the Portuguese Foundation for Science and Technology (FCT), under research project PTDC/ECM/114189/2009, and by QREN, the Operational Programme for Competitiveness Factors, under the research project Active Floor Project (FCOMP-01-0202-FEDER-021583).

7. References

[1] European Commission, Directive 2010/31/EU, Energy Performance of Building Directive, 2010.

[2] G. Manioglu, Z. Yilmaz, Economic evaluation of the building envelope and operation period of heating system in terms of thermal comfort, Energy and Buildings 38:3 (2006) 266-272.

[3] C. D. Pereira, E. Ghisi, The influence of the envelope on the thermal performance of ventilated and occupied houses, Energy and Buildings 43:12 (2011) 3391-3399.

[4] A. Tadeu, I. Simões, N. Simões, J. Prata, Simulation of dynamic linear thermal bridges using a boundary element method model in the frequency domain, Energy and Buildings 43:12 (2011) 3685-3695.

[5] I. Simões, N. Simões, A. Tadeu, Thermal delay simulation in multilayer systems using analytical solutions, Energy and Buildings 49 (2012) 631–639.

[6] F. Mathieu-Potvin, L. Gosselin, Thermal shielding of multilayer walls with phase change materials under different transient boundary conditions, International Journal of Thermal Sciences 48:9 (2009)1707-1717.

[7] Z. Yilmaz, Evaluation of energy efficient design strategies for different climatic zones: Comparison of thermal performance of buildings in temperate-humid and hot-dry climate, Energy and Buildings 39:3 (2007) 306–316.

[8] K. A. Antonopoulos, E. P. Koronaki, Thermal parameter components of building envelope, Applied Thermal Engineering 20:13 (2000) 1193-1211.

[9] N. Aste, A. Angelotti, M. Buzzetti, The influence of the external walls thermal inertia on the energy performance of well insulated buildings, Energy and Buildings 41:11 (2009) 1181-1187.

[10] J. M. Roucoult, O. Douzane, T. Langlet, Incorporation of thermal inertia in the aim of installing a natural nighttime ventilation system in buildings, Energy and Buildings 29:2 (1999) 129-133.

[11] J. Pfafferott, S. Herkel, J. Wapler, Thermal building behavior in summer: long-term data evaluation using simplified models, Energy and Buildings 37 (2005) 844-852.

[12] L. E. Mavromatidis, M. EL Mankibi, P. Michel, M. Santamouris, Numerical estimation of time lags and decrement factors for wall complexes including Multilayer Thermal Insulation, in two different climatic zones, Applied Energy 92 (2012) 480-491.

[13] K. A. Antonopoulos, C. Tzivanidis, A correlation for the thermal delay of buildings, Renewable Energy 6:7 (1995) 687-699.

[14] K. A. Antonopoulos, E. P. Koronaki, Effect of indoor mass on the time constant and thermal delay of buildings, International Journal of Energy Research 24:5 (2000) 391-402.

[15] E. D. Kravvaritis, K. A. Antonopoulos, C. Tzivanidis, Experimental determination of the effective thermal capacity function and other thermal properties for various phase change materials using the thermal delay method, Applied Energy 88:12 (2011) 4459-4469.

[16] F. Alhama, J. F. López-Sánchez, C. F. González-Fernández, Heat conduction through a multilayered wall with variable boundary conditions, Energy 22:8 (1997) 797–803.

[17] A. Tadeu, J. António, D. Mateus, Sound insulation provided by single and double panel walls – a comparison of analytical solutions versus experimental results, Applied Acoustics 65 (2004) 15-29.

[18] T. E. Vigran, Sound transmission in multilayered structures – Introducing finite structural connections in the transfer matrix method, Applied Acoustics 71 (2010) 39–44.

[19] K. Yagi, K. Halada, Materials development for a sustainable society, Materials & Design 22 (2001) 143-146.

[20] A. Mestre, L. Gil, Cork for Sustainable Product Design, Ciência e Tecnologia dos Materiais 23:3/4 (2011) 52-63.

[21] F. Hernandez-Olivares, M. R. Bollati, M. del Rio, B. Parga-Landa, Development of cork gypsum composites for building applications, Construction and Building Materials13 (1999) 179-186.

[22] S. P. Silva, M.A. Sabino, E. M. Fernandes, V. M. Correlo, F. L. Boesel, R. L. Reis, Cork: properties, capabilities and applications, International Materials Reviews 50:6 (2005) 345-365.

[23] C. Pereira, F. C. Jorge, M. Irle, J. M. Ferreira, Characterizing the setting of cement when mixed with cork, blue gum, or maritime pine, grown in Portugal I: temperature profiles and compatibility indices, Journal of Wood Science 52 (2006) 311-317.

[24] L. Gil, P. Silva, Characterization of Insulation Corkboard Obtained from Demolitions, Ciência e Tecnologia dos Materiais 23:3/4 (2011) 2-9.

[25] O. Castro, J. M. Silva, T. Devezas, A. Silva, L. Gil, Cork agglomerates as an ideal core material in lightweight structures, Materials & Design 31 (2010) 425-432.

[26] K. T. Huang, H. H. Liang, M. J. Hun, Improvement in fire prevention performance of cork-gypsum decorative materials by applying porous waste, International Journal of Physical Sciences 5:12 (2010) 2038-2044.

[27] E. M. Fernandes, V. M. Correlo, J. A. M. Chagas, J. F. Mano, R. L. Reis, Properties of new cork–polymer composites: Advantages and drawbacks as compared with commercially available fibreboard materials, Composite Structures 93 (2011) 3120-3129.

[28] A. Mir, B. Bezzazi, R. Zitoune, F. Collombet, Study of mechanical and hygrothermal properties of agglomerated cork, Mechanika 18:1 (2012) 40-45.

[29] M. A. Azziz, C. K. Murphy, S. D. Ramaswamy, Lightweight concrete using cork granules, International Journal of Cement Composites and Lightweight Concrete 2:1 (1979) 29-33.

[30] S. R. Karade, M. Irle, K. Maher, Influence of granule properties and concentration on cork-cement compatibility, Holz als Roh- und Werkstoff 64 (2006) 281–286.

[31] N. Simões, I. Simões, A. Tadeu, C. A. B. Vasconcellos, W. J. Mansur, 3D Transient Heat Conduction in Multilayer Systems - Experimental Validation of Semi-analytical Solution, International Journal of Thermal Sciences 57 (2012) 192-203.

[32] D. Maillet, S. André, J. C. Batsale, A. Degiovanni, C. Moyne, Thermal Quadrupoles: Solving the Heat Equation through Integral Transforms, Wiley, 2000.

[33] A. Joanni, E. Kausel, Heat diffusion in layered media via the thin-layer method, International Journal for Numerical Methods in Engineering 78:6 (2009) 631-756.

[34] International Organization for Standardization, ISO 8302: Thermal insulation – Determination of steady-state thermal resistance and related properties – Guarded hot plate apparatus (1991).

[35] European Standards, EN 12667: Thermal performance of building materials and products. Determination of thermal resistance by means of guarded hot plate and heat flow meter methods. Products of high and medium thermal resistance (2001).

[36] European Standards, EN 1602: Thermal insulating materials, Thermal insulation, Construction materials, Density measurement, Bulk density, Test specimens, Testing conditions, Buildings (1996).

[37] Portuguese Standards, NP EN 12390-7:2009. Testing hardened concrete. Part 3: Compressive strength of test specimens. Ed. 2 2009.

Figures' Captions

Figure 1: Geometry of the problem.

Figure 2: Analytical and experimental results for the thermocouples at the layer interfaces and within the test specimen M150 (System 1) simulating 1D heat conduction.

Figure 3: Composition and dimensions of the floor systems studied: a) Case 1 - a concrete slab covered with a screed or ICB layer; b) Case 2 – a concrete slab covered with a screed or ICB layer and an additional floating layer, 30 mm thick ; c) Case 3 - a concrete slab covered with a 30 mm layer of screed, and an ICB layer; d) Case 4 - a concrete slab covered with a 30 mm layer of screed, an ICB layer and an additional floating layer, 30 mm thick.

Figure 4: Evaluation of the heat source.

Figure 5: Analytical results for Example 1 when the lightweight screed (M150) is 60 mm thick, with definition of the thermal delay (T2 –T1).

Figure 6: Thermal delay (solid lines) and thermal transmittance coefficient (dashed lines), U, of each multilayer system: a) Case 1 incorporated an ICB or a LWS layer; b) Case 2 incorporated an ICB or a LWS layer; c) Case 3 incorporated an ICB or a LWS layer; d) Case 4 incorporated an ICB or a LWS layer; e) Case 1 incorporated a reference screed layer; f) Case 2 incorporated a reference screed layer; g) Case 3 incorporated a reference screed layer; h) Case 4 incorporated a reference screed layer.

Table 1: Lightweight screed compositions

Sample	Cement ($kg.m^{-3}$)	Sand ($kg.m^{-3}$)	ECG 3/5 ($kg.m^{-3}$)	ECG 5/10 ($kg.m^{-3}$)	Water ($kg.m^{-3}$)
M150	151.1	377.7	27.9	32.5	81.4
M250	254.6	358.3	25.5	29.8	138.8
M400	400.0	339.8	26.9	31.5	202.2
R150	156.9	1488.0	-	-	105.4
R250	253.9	1302.2	-	-	119.8
R400	401.0	1448.2	-	-	178.3

Table 2: Thermal conductivity and mass density and measurement uncertainties

Material	Thermal conductivity[(1)], λ ($W.m^{-1}.^{o}C^{-1}$)	Mass density[(1)], ρ ($kg.m^{-3}$)
Moulded Expanded Polystyrene (EPS)	$0.041 \pm 7.5x10^{-4}$	14.3 ± 0.233
Agglomerate of Expanded Cork (ICB)	$0.038 \pm 6.5x10^{-4}$	100.0 ± 0.433
M150	$0.195 \pm 5.2x10^{-3}$	520 ± 4.992
M250	$0.214 \pm 5.6x10^{-3}$	740 ± 7.104
M400	$0.318 \pm 7.9x10^{-3}$	900 ± 8.640
R150	$0.677 \pm 16.2x10^{-3}$	1580 ± 15.168
R250	$0.699 \pm 16.7x10^{-3}$	1600 ± 15.360
R400	$0.783 \pm 18.7x10^{-3}$	1980 ± 18.912

(1) average values of three tested specimens

Table 3: Multilayer systems tested to determine the specific heat

System 1		System 2		System 3		System 4		System 5		System 6	
Layer	**(mm)**	**Layer**	**(mm)**	**Layer**	**(mm)**	**Layer**	**(mm)**	**Layer**	**(mm)**	**Layer**	**(mm)**
EPS	9.67	**EPS**	9.67	**EPS**	9.67	**EPS**	9.67	**EPS**	9.58	**EPS**	9.58
M150	97.10	**M250**	92.60	**M400**	94.90	**R150**	97.90	**R250**	98.30	**R400**	97.10
EPS	9.57	**EPS**	9.57	**EPS**	9.57	**EPS**	9.57	**EPS**	9.55	**EPS**	9.55

Table 4: Specific heat and thermal diffusivity

Material	Specific heat, c ($J.kg^{-1}.^oC^{-1}$)	Thermal diffusivity, $\alpha = \lambda / (\rho c)$ ($m^2.s^{-1}$)
Moulded Expanded Polystyrene (EPS)	1430.0	2.16e-07
Agglomerate of Expanded Cork (ICB)	1560.0	2.44e-07
M150	950.0	3.95e-07
M250	720.0	4.02e-07
M400	700.0	5.05e-07
R150	900.0	4.76e-07
R250	850.0	5.14e-07
R400	750.0	5.27e-07

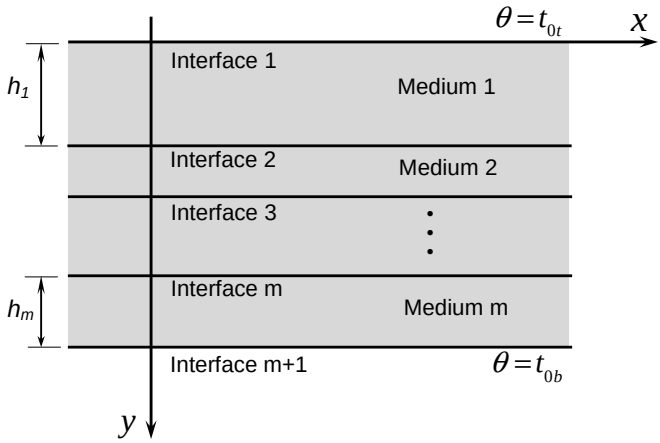

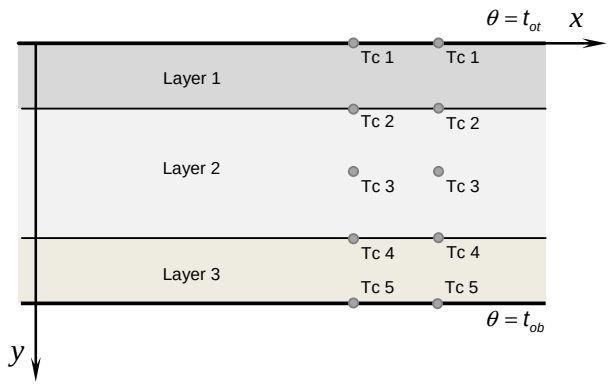

Thermocouple positions (mm)	
TC 1	$y = 0$
TC 2	$y = 10$
TC 3	$y = 55$
TC 4	$y = 106$
TC 5	$y = 116$

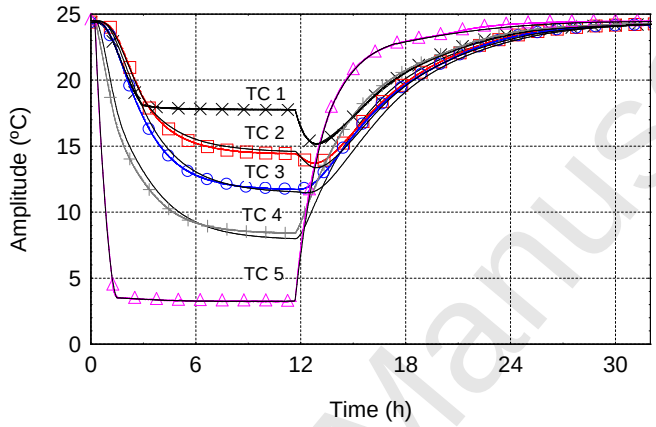

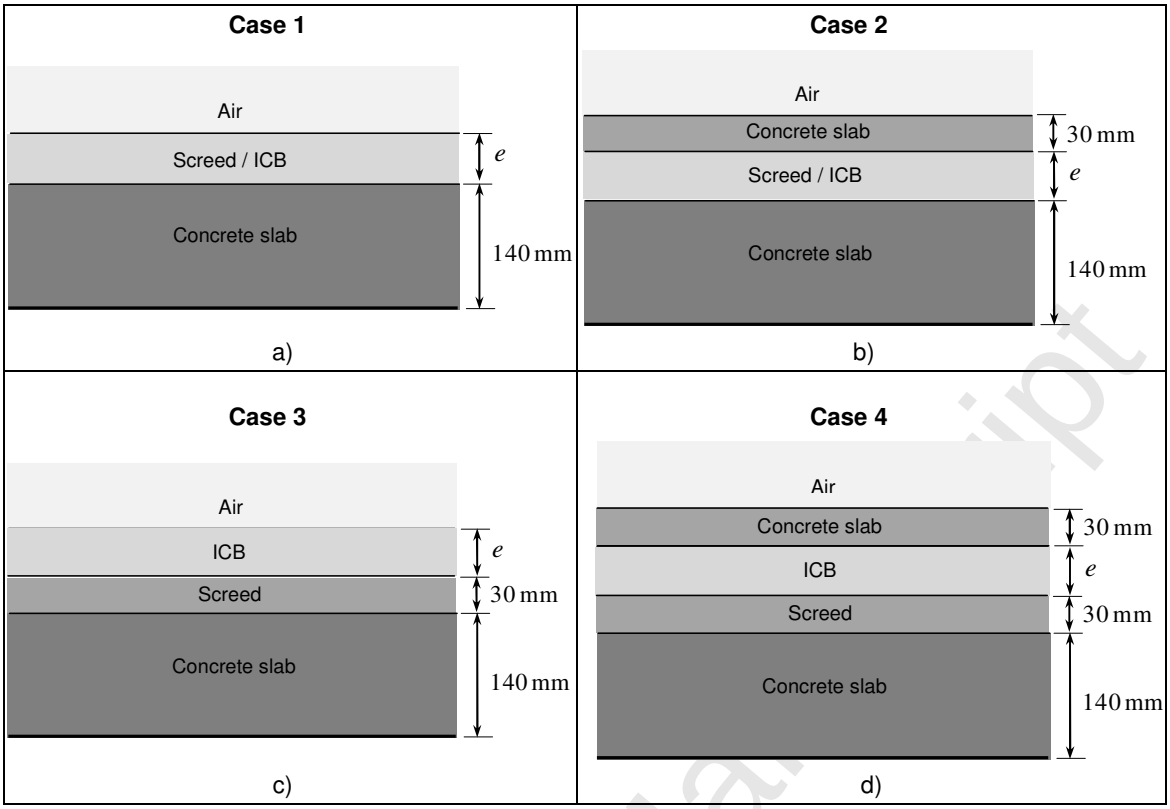

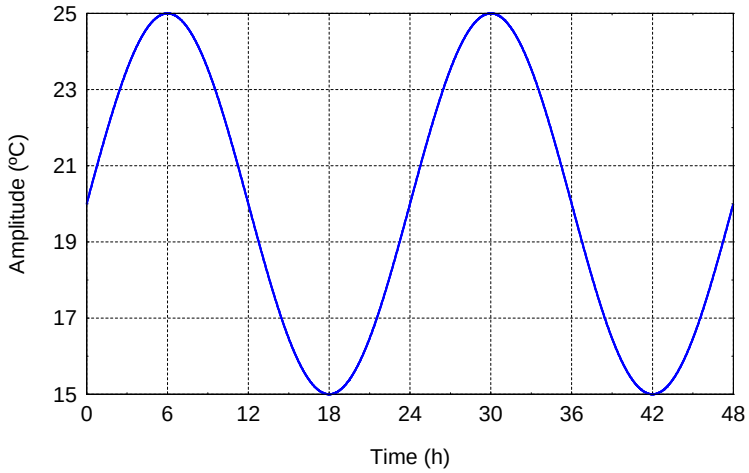

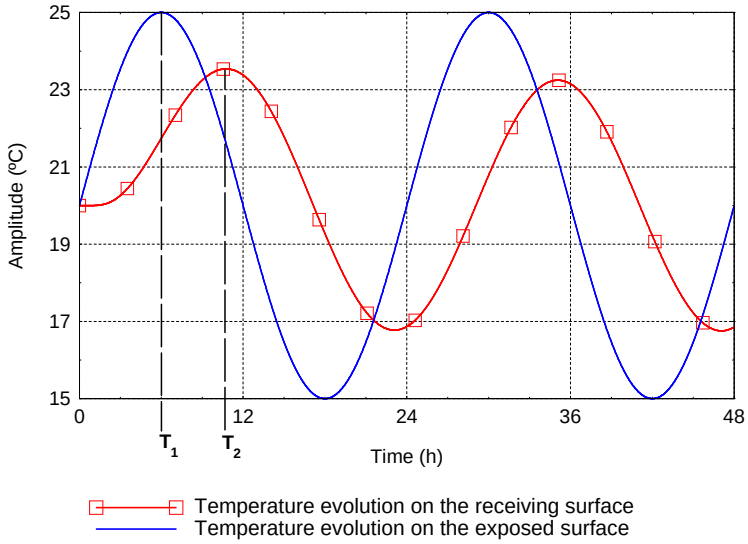

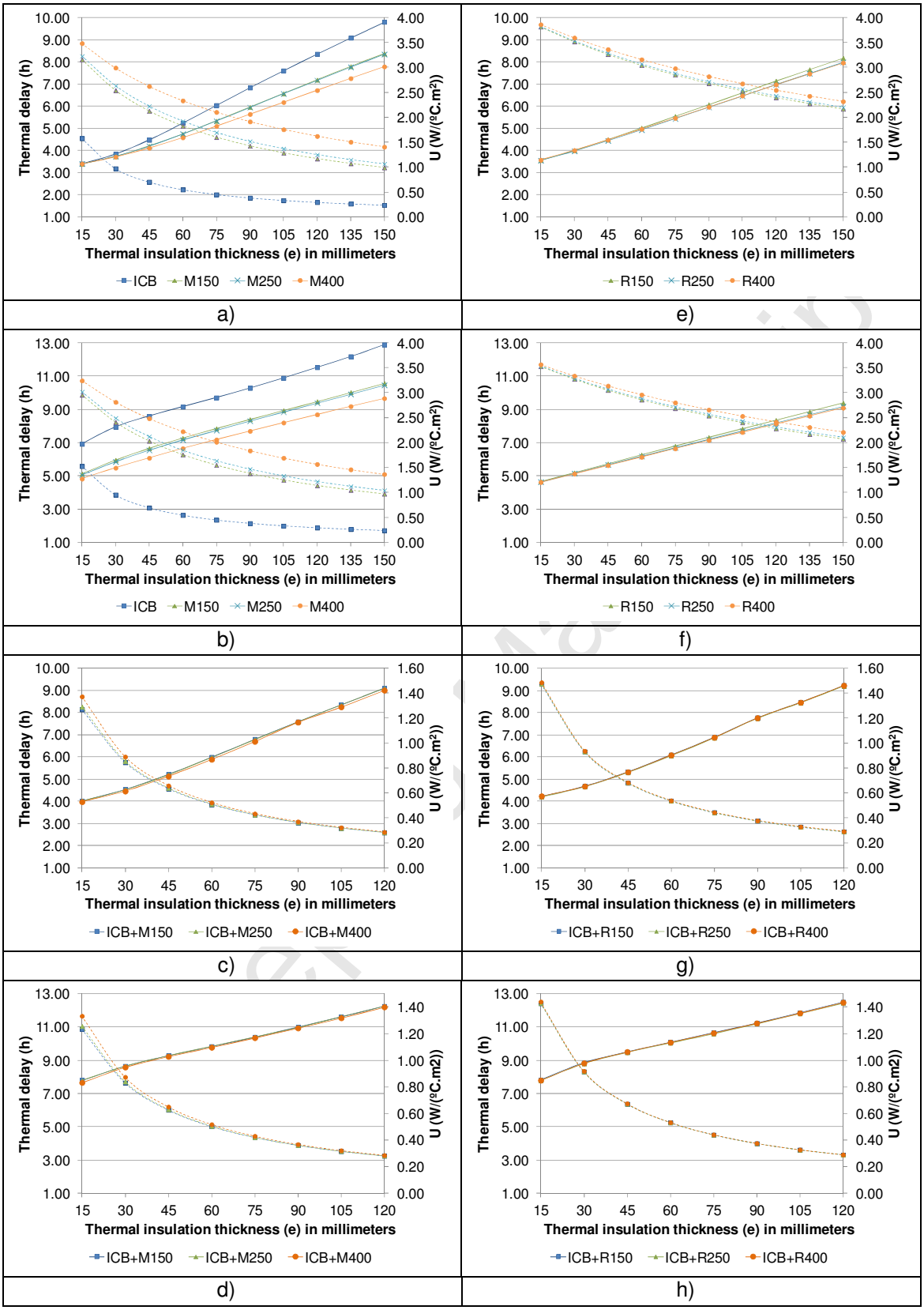

Highlights

The thermal delay of concrete floors built with cork's layers and screed with cork.

The heat transfer by conduction across multilayer systems is simulated analytically.

The system is computed in the frequency domain assuming unsteady boundary conditions.

The material's properties are more relevant to thermal lag in systems with few layers.

Longer thermal delays were found in the system built with a greater number of layers.